

Chapter-I

Nanocrystalline Ferrites

CHAPTER- I

NANOCRYSTALLINE FERRITES

1.1 Introduction

Nanocrystalline spinel ferrites have been investigated in the recent years by many authors [1-8]. There are several methods of preparing these ferrite materials. The basic theme of all these is to energize the materials to a highly non-equilibrium state through melting, evaporation, irradiation, applications of pressure, storing of material energy etc. [9].

Many researchers have reported the important dielectric properties of Li ferrite [10-12]. Because of the low loss and improved dielectric properties it is used a microwave material. Lithium ferrite occupies a prominent position among other ferrites (magnetic materials)

1.2 Structure of ferrite

The structure of the cubic spinel ferrite is determined by a closed packed structure of oxygen ions. These are assumed to be rigid spheres of ionic radius $r_o = 1.38 \text{ \AA}$. Some of the remaining hollow spheres are occupied by the smaller metal ions with $r_{me} = 0.6 \text{ to } 1.0 \text{ \AA}$. The hollow spaces available in an ideal close-packed structure of rigid oxygen anions would be able to incorporate on tetrahedral sites only ions with maximum radius $r_{tetra} < 0.30 \text{ \AA}$ and on octahedral sites only ions with maximum radius $r_{oct} < 0.55 \text{ \AA}$. This

would result in a cell edge $a = 7.47 \text{ \AA}$. To incorporate the cations mentioned above the lattice has to be expanded. Somewhat the difference in expansion of the tetrahedral and octahedral interstices is characterized by an oxygen parameter u . The distance between the tetrahedral site $(0, 0, 0)$ and oxygen site $(3/8, 3/8, 3/8)$ is $u_{\text{ideal}} = 3/8 = 0.375 \text{ \AA}$. u_{obs} is always larger than u_{ideal} , resulting the greater expansion of the tetrahedral interstices at the expense of octahedral sites.

The ferrites have the general formula $[M_{4-x}Fe_x] [M_xFe_{2-x} O_4]$. The divalent metal element M (Mg, Zn, Mn, Fe, Co, Ni etc) can occupy either tetrahedral (A) or octahedral (B) sites in the cubic structure. The unit cell contains 8 formula unit of MFe_2O_4 . Hence the unit cell formula is $M_8^{2+}Fe_{16}^{3+}O_{32}^{2-}$. The 32 oxygen ions from two kinds of interstitial sites, tetrahedral or A-site [four oxygen neighbors] and octahedral or B-sites [six oxygen neighbors] per unit cell. Out of these, 8 tetrahedral and 16 octahedral sites are occupied by the cations.

The spinel structure A-site and B-site arrangements are shown in Fig. 1.1 and 1.2.

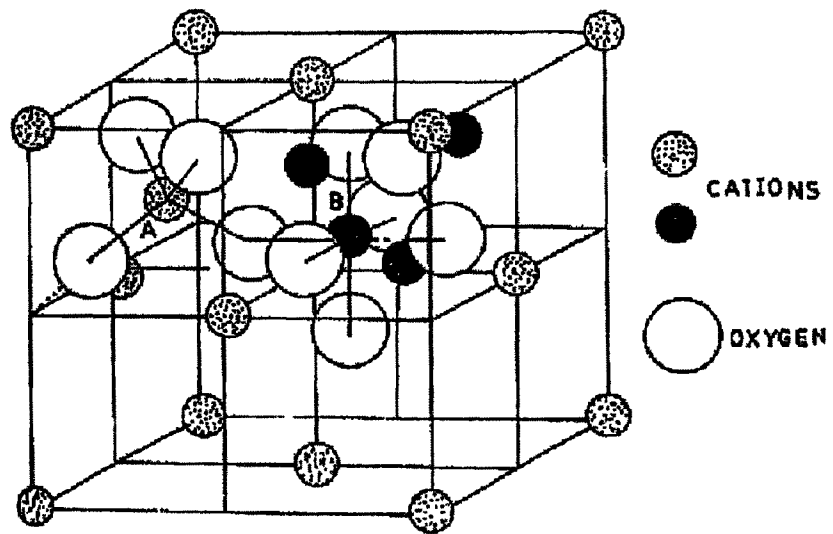


Fig. 1.1 - Spinel structure

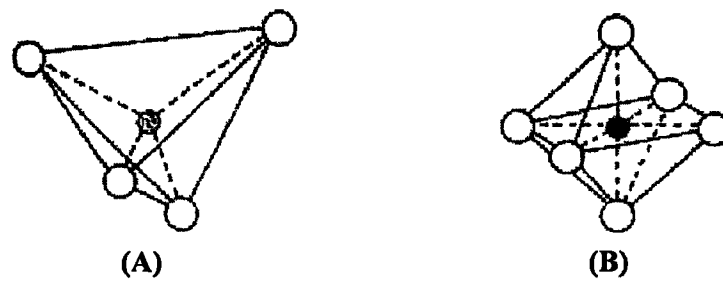


Fig. 1.2 - Tetrahedral (A) and Octahedral (B) sites

1.3 Classification of nanocrystalline materials

Nanomaterials are classified as nanostructure materials and nanoparticle materials. The size of nanoparticle covers the wide range of 1–200 nm. On the basis of modulation nature, nanocrystalline materials are classified as,

i. The nanocrystalline materials are single phase or multiphase polycrystals, which are based on modulation dimensionality. The crystal size is of the order of few nanometers in at least one dimension.

a) Three-dimensional ($\mu = 3$)

When nanocrystalline materials are equiaxed in nature they are termed as nanostructure crystallites or three-dimensional.

b) Two-dimensional ($\mu = 2$)

When they are filamentary in nature, they are termed as two-dimensional.

c) One-dimensional ($\mu = 1$)

When they consist of a lamellar structure, they are termed as layered nanostructure or one-dimensional.

d) Zero-dimensional ($\mu = 0$)

They are atoms, cluster or cluster assemblies. Rieke and his coworkers have proposed the classification of nanocrystalline materials on the

basis of the correlation between morphology and magnetic properties.

These four types are

- a) **Type A:** The ultra fine particle with large interparticle spacing to have the non-interacting magnetic particles. Ferro fluids belong to this category since the magnetic particles are surrounded by surfactant which prevents the interparticle interaction in the fluid. The magnetic properties are due to the small number of non interacting magnetic particles with practically no contribution from their mutual interaction.
- b) **Type B:** Materials include fine particles with a core shell are included in this type .In type B the shell core may prevent the particle interaction but the core shell interaction are possible mainly, because the shell are formed due to oxidation of core particles and these are magnetic.
- c) **Type C:** Nanocomposites composed of small magnet particles embedded in chemically dissimilar matrix e.g. Ni-Zn ferrite in glass matrix. In this type magnetic interactions are decided by the volume fraction of the magnetic particles present in the matrix.
- d) **Type D:** In this class, material consists of small crystallites dispersed in non-crystalline matrix of identical second phase materials e.g. nanosized powder of Fe_2O_3 . These types of materials are bulk materials with nanocrystalline structure. The magnetic behaviour of these materials is a result of the contributions from both interparticle interaction and the size effects.

1.4 Properties of substituted Li- ferrites

1.4.1 Dielectric behavior

Ferrites have abnormally high dielectric constant and show dispersion of dielectric constant with frequency. The dielectric loss is due to inhomogeneous dielectric structure. The sintering temperature and sintering techniques can control the dielectric behavior and also the resistivity of the ferrite materials. The oxygen atmosphere creates insulating layers on the conduction grains, these conducting grains separates low conducting grains. Hence the conductivity of ferrite is very low.

1.4.2 Electrical conductivity

The resistivity of ferrites varies from 10^{-3} ohm \cdot cm to 10^{11} ohm \cdot cm. The Fe^{2+} ions are responsible for conduction and amount of Fe^{2+} ions in ferrite are dependent on the sintering temperature and impurities, porosity and rate of cooling. High resistivity oxide materials change their resistivity by addition of other foreign oxides. The conductivity of the ferrite is also associated with the addition of metal ions with more than one valance state [13, 14].

1.4.3 Magnetization

Lithium ferrite is inverse spinel ferrite. The Fe^{3+} ions on A site are coupled with their spin anti-parallel Fe^{3+} ions on B site, so that the net moment is only due to divalent M^{2+} ions. In pure Lithium ferrite $4\pi Ms$ is ~ 3750 Gauss at room temperature. This value is changed by substitution of other ions. The substituted lithium ferrites were prepared with their $4\pi Ms$ changed in the

range of few hundred Gauss to five thousand Gauss. The magnetization is the temperature dependent, as temperature increases magnetization decreases and it becomes zero at Curie temperature. The Curie temperature of pure lithium ferrite is ~ 640 °C. The Curie temperature decreases due to substitution.

1.4.4 Hysteresis behavior

The square -loop characteristic of ferrite has applications in computer memory and also in logic devices. The lithium ferrite is employed in latching microwave devices, because of its high remanence ratio and low coercive force.

1.5 Properties of nanocrystalline ferrites

Ferrites have vast applications from microwaves to radio frequencies. They possess very low conductivity which is one of the considerations for microwave applications. The small particle size ferrites have remarkable properties such as increased strength, enhanced diffusivity, improved ductility, reduced density, reduced elastic modulus, higher electrical resistivity, increased specific heat, higher thermal expansion coefficient, lower thermal conductivity and superior soft properties in comparison to conventional coarse grained materials.

1.5.1 Strength and hardness

A decrease in the grain size significantly affects yield strength and hardness [15]. The grain boundary structure, boundary angle, boundary sliding and movement of dislocation are important factors that determine the

mechanical properties of nanostructure materials. An enhancement in damping capability of nanostructured solid may be associated with grain boundary sliding [16]. The elastic constant of nanocrystalline materials have found to be reduced 30% or less. The reduction in Young's modulus value interpreted by others [17] is due to level of porosity and state of cracks in the samples.

1.5.2 Specific heat

Specific heat of materials is closely related to its vibrational and configurationally entropy, which is significantly affected by the nearest neighbour configurations. The increase in specific heat of nanocrystalline materials has been attributed to reduce the grain growth [18].

1.5.3 Thermal expansion

A thermodynamic property such as thermal expansion coefficient is closely related to the grain size. Measured thermal expansion coefficient of nanocrystalline Cu, Pd, Fe-B-Si and Ni-P alloys were almost twice the value for single crystal [19-21]. Different preparation methods, preparation conditions, sintering temperature etc. can tailor the predetermined values of thermal expansion coefficient of nanocrystalline materials. The melting temperature of Au particles drops to as low as 300 °C for particles with diameter smaller than 5 nm much lower than the bulk melting temperature 1063 °C for Au [22].

1.5.4 Ductilization of ceramics and intermetallics

The finite grain size and high rate of diffusivity observed in nanocrystalline materials suggest that considerable ductility can occur in these materials even at room temperature. Thus the diffusional creep rate of polycrystalline sample can be increased by reducing the grain size and /or by increasing the grain boundary diffusivity. The grain size of nanocrystalline material is reduced by three orders of magnitude compared to conventional polycrystalline materials (from about 10 μm to nm) and the boundary diffusivity is higher by three orders of magnitude. Accordingly, nanocrystalline ceramic intermetallic compounds are generally expected to exhibit a 12 order of magnitude increase in diffusional creep [23]

1.5.5 Magnetic properties

The ferromagnetic properties of nanocrystalline materials are influenced by particle size change in interatomic distance. Thus the saturation magnetization (M_s) and ferrimagnetic transition temperature of nanocrystalline materials are considerably reduced with respect to the bulk materials. The M_s of 6 nm-irons is 130 emu/g [24], while that of normal polycrystalline α -Fe is 220 emu/g and that of iron-based metallic glasses is 215 emu/g. Unlike the bulk ferromagnetic materials which usually form multiple magnetic domains. The average values σ_s and H_c can be correlated with the annealing temperature. The domain structure develops as the diameter of nanocrystallites exceeds the critical diameter that corresponds to single

domain state. In case of single domain nanocrystallites the surface spins are ferrimagnetically aligned [25]. The surface effects are the results of finite size scaling of nanocrystalline, which in turn leads to non-co-linearity of magnetic moments on their surface. The bulk ferrimagnetic materials which usually form multiple magnetic domains several small ferromagnetic particles could consists of only single magnetic domain. In the case of single particle being a single domain, the super paramagnetism occurs in which the magnetization of particles are randomly distributed and they are aligned only under an applied magnetic field and the alignment disappears once the external field is withdrawn.

In the spherical particle model, the critical diameter $(D_c)_{\text{teor}}$ (below which the particle is considered single domain) can be calculated with the following formula [26]

$$(D_c)_{\text{teor}} = \frac{9E_p}{2\pi M_s^2} \quad \text{---- 1.1}$$

where E_p is the density energy of the magnetic domain wall and M_s is the spontaneous magnetization.

As compare to the bulk materials, the saturation magnetization of nanocrystalline materials gets reduced. Similarly a reduction in the Curie temperature (T_C) of nickel ferrite by about 40 °C is reported. These reductions were attributed to the deviation of interatomic spacing in the interfacial region

as compared to crystalline component supported by Mossbauer spectroscopy measurement.

The large surface to volume ratio results in different local environment for surface atoms leading to the mixed volume and surface magnetic characteristics.

When the material containing extremely small magnetic particulates in a non-magnetic or weakly magnetic matrix is placed in magnetic field, the magnetic spins of the particulates tends to align with the field. This increase in magnetic order lowers the magnetic entropy of spin system. If this process is performed adiabatically, no heat is exchanged with surrounding the temperature of the specimen will rise. This temperature rise is reversible (the specimen cools with on removal of magnetic field) and is known as the magnetocaloric effect.

1.6 Literature survey of nanocrystalline ferrites.

Lot of work has been carried out recent in nanocrystalline magnetic materials. Spinel related magnesium $\text{Li}_{0.5}\text{Fe}_{2.5}\text{O}_4$ has been synthesized by heating magnesium substituted corundum-related $\alpha\text{-Fe}_2\text{O}_4$ with Li_2CO_3 at $600\text{ }^\circ\text{C}$ [27]. Magnetic and electric properties of nanocrystalline ferrite depend upon cation distribution in the spinel structure [28].

Electrical conductivity and dielectric measurements have been performed for nanocrystalline NiFe_2O_4 with average grain size ranging between 8 to 97 nm [29].

Chatterjee et. al. (1990) have studied the Mössbauer spectra of nano-composites in the system (Fe-Cr)-SiO₂ prepared by sol-gel method followed by suitable reduction treatment. The spectra consist of a weak sextet pattern with hyperfine field around 328 kOe attributed to the presence of α - iron [30]

Tang et. al. (1991) have reported the behavior of magnetic transition temperature when the system dimensions are reduced. Nanocrystalline MnFe₂O₄ particles in the size range of 7.5 to 24.5 nm have been prepared by a chemical process. Studies show that the Curie temperature (T_c) increases when the particle size is reduced to nanoscale range [31].

Magnetic properties at low temperature for nanocrystalline Ni-Zn ferrite in a borate glass matrix prepared by the glass ceramic route have been reported by Pal et al [32].

Metastable nanocrystalline nickel ferrite (NiFe₂O₄) with crystallite size ~ 9 nm produced by high energy milling. X-ray diffraction, thermogravimetric measurements, Mössbauer spectroscopy, electron microscopy and magnetization experiments have been used to investigate the changes induced in the microstructure and magnetic properties [33].

The magnetization studies on nanocrystalline nickel ferrite as powder particles and as diluted dispersion (10 wt %) in polymer matrix are presented. The two polymer based nanocomposites were prepared via ball milling and in situ polymerization respectively [34]. The reverse micelle approach has been

extended to synthesize nanocrystalline ferrites with varying surface roughness of 8-18 Å [35].

Nanocrystalline $\text{Ni}_{0.35}\text{Zn}_{0.65}\text{Fe}_2\text{O}_4$ mixed ferrite was obtained from the $\text{Fe}_2(\text{Ni}_{0.35}\text{Zn}_{0.65})(\text{OH})_4(\text{C}_2\text{H}_2\text{O}_4)_2 \cdot \text{H}_2\text{O}$ complex combination decomposed at 325 °C and these mixtures was annealed in the temperature range 400-1000 °C for 2 h. The thermal analysis of the synthesized complex combination was done by TG-DTA techniques [36].

High permeability soft magnetic materials are nanocrystalline alloys. VITROPREM is the most prominent new alloys [37, 38] produced by rapidly quenching techniques, low cost raw materials and consequences of zero magnetostriction. Nanocrystalline ferrite formation by ball milling in $\text{Fe}_{0.89}\text{C}$ spheroidite steel and its annealing behavior have been studied through the microstructure observation and micro hardness measurements. It was found that the dislocation density increases and dislocation cells form due to plastic deformation [39].

The single-phase zinc ferrite was prepared through a single step low temperature reaction by the liquid phase deposition (LPD) method and this ferrite was characterized by TGA and EDX measurements [40].

Three-dimensional structure of nanocrystalline magnesium ferrite MgFe_2O_4 was prepared by ball milling has been determined using synchrotron radiation power diffraction and employing both Rietveld and atomic pair distribution function (PDF) analysis [41].

Highly crystalline nickel ferrite films with different chemical compositions were processed via spin spraying method and their morphological structural and magnetic properties were subsequently investigated [42].

The effect of annealing on the magnetic properties of nanocrystalline ZnFe_2O_4 has been studied. The sample ZnFe_2O_4 is prepared with particle size of about 3 nm. The particle size significantly increases on annealing [43].

Nanocrystalline nickel and zinc ferrites were synthesized using micro emulsion technique and characterized by high-resolution transmission electron microscopy and vibrating sample magnetometry [44].

Ni-Zn nanocomposite with copolymer matrix formaldehyde in the presence of varying concentration of zinc ions have been studied at room temperature and normal pressure. The band gap of these materials is determined by reflection spectra [45].

1.7 Application of nanocrystalline materials

Nanocrystalline materials possess unique, beneficial chemical, physical and mechanical properties. They can be used for a wide variety of applications.

1) Chokes for radio frequency

The design of common mode chokes for radio frequency interference filter is considered in most of places of industrial and domestic power supplies (SMPS) [46]. It clearly points out that volume of the core can be reduced by

50 to 80%, when appropriate ferrites are replaced by well chosen nanocrystalline core as a result of its superimposed advantages of high and tailored permeabilities, high saturation and inductive behavior near CMC resonance.

2) High power magnets

The strength of a magnet is measured in terms of coercivity and saturation magnetization values. The values depends on grain size and increase in specific surface area (surface area per unit volume of the grains) of the grains. It has been shown that magnet made of nanocrystalline yttrium-Samarium-cobalt grains posses very unusual magnetic properties due to their extremely larger surface area. Typical applications for these high power rare-earth magnets are in submarines, automobile alternators, land based power generators motors for ships, ultra sensitive analytical instruments and magnetic resonance imaging in medical diagnostics.

3) Better insulation materials

Nanocrystalline materials synthesized by sol-gel techniques are porous and extremely light weight and are used as materials for 'smart' windows.

4) Phosphors for high definition TV

The resolution of a television, or a monitor, depends greatly on the size of the pixel. These pixels are essentially made of materials called "phosphors" which glow when struck by a stream of electrons inside of the pixel, or the

phosphors. Nanocrystalline zinc selenide, zinc sulfide, cadmium sulfide and lead telluride synthesized by the sol-gel techniques.

5) Tougher and harder cutting tools

Cutting tools made of nanocrystalline materials such as tungsten carbide, tantalum carbide and titanium carbide are much harder, much more wear-resistant, erosion-resistant, and last longer than their conventional counterparts.

6) Elimination of pollutants

Nanomaterials are very active in terms of their chemical, physical and mechanical properties. Due to their enhanced chemical activity, nano materials can be used as catalysts to react with such noxious and toxic gases as CO, NO₂. The synthesis of mesoporous materials can be useful for environmental cleaning [47].

7) High energy density batteries

The storage capacity of the conventional and rechargeable batteries used in laptops, electric vehicles, cellular phones, cordless phones, toys and watches are quite low requiring frequent recharging. Nanocrystalline materials synthesized by sol-gel techniques are candidates for separator plates in batteries, because their foam-like structure can hold more energy than conventional one.

8) Magnetic nanocrystalline materials for information storage

Magnetic nanocrystalline materials have important applications such as in color imaging [48], bioprocessing [49], magnetic refrigeration [50] and ferro fluids [51]. Information storage depends on the size of domains.

Nanocrystalline spinel ferrites have the applications in non-resonant devices, radio frequency circuits, high quality filters, rod antennas, transformer cores, read/write heads for high speed digital tapes operating device etc. [52-57].

1.8 Orientation of the problem

Lithium ferrite is the most widely used ferrite because of its rectangular square hysteresis loop characteristics. It is expected that the magnetic and electric properties could get modified in its nanocrystalline form with diatomic Ni^{2+} .

There are number of reports in the literature on the studies of Li-Zn, Li-Cd, Li-Mg, Li-Zn-Ti and Li-Mg-Ti ferrites by ceramic method. The effect of substitution of Ni^{2+} in lithium ferrite on the electrical and magnetic properties in nanocrystalline ferrites $\text{Li}_{0.5}\text{Ni}_{1.5x}\text{Fe}_{2.5-x}\text{O}_4$, ($x = 0.1, 0.2, 0.3, 0.4$ and 0.5) is studied. In this present work it is prepared by chemical route.

The present research work involved -

1. Preparation of $\text{Li}_{0.5}\text{Ni}_{1.5x}\text{Fe}_{2.5-x}\text{O}_4$ ferrite by chemical method.

2. X-ray diffraction studies to confirm the formation of the spinel phase and calculation of lattice parameter, site radii and bond length etc.
3. Study of microstructural aspects with the help of SEM.
4. IR studies to detect the internal vibration due to tetrahedral and octahedral metal complexes.
5. Studies on electrical properties such as dc resistivity, dielectric constant, $\tan \delta$ etc.
6. Studies on magnetic properties such as the magnetization, magnetic moment and ac susceptibility etc.

References

- 1 J. S. C. Jang and C. C. Koch
Scri. Mater. 24 (1990) 1599-1604
- 2 S. Takaki and Y. Kimura
J. Jpn. Soc. Powder and Metal. 46 (1999) 135-1240
- 3 J. Yin, M. Umemoto, Z. G. Liu and K. Tsuchiya
ISI J. Int. 41 (2001) 1389-1396
- 4 H. H. Tian and M. Atsmon
Acta. Mater. 47 (1999) 1255-1261
- 5 Y. H. Zhao, H. W. Sheng and K. Lu
Acta. Mater. 49 (2001) 365.375
- 6 Z. G. Liu, X. J. Hao, K. Masuyama, K. Tsuchiya, M. Umemoto and S. M. Hao
Scri. Mater. 44 (2001) 1775-1779
- 7 M. Umemoto, Z. G. Liu, X. J. Hao, K. Masuyama and K. Tsuchiya
Mater. Sci. Forum. 360-362 (2001) 167-174
- 8 M. Umemoto, Z. G. Liu, Y. Xu and K. Tsuchiya
Mater. Sci. Forum. 386-388 (2002) 323- 328
- 9 D. Turnbull
Met. Trans. A 12695 (1981)
- 10 T. Colins and A. E. Brown
J. Appl. Phys. 42(1971) 3451
- 11 A. M. Shaikh.
Ph.D. Thesis, Shivaji Univ., Kolhapur (1998)
- 12 M. G. Patil
Bull. Mater. Sci. 17 (1994) 399
- 13 E. J. W. Verwey and J. H. deBoer
Reclav Chem. Phys. Bas. 55 (1936) 531

- 14 E. J. W. Verwey, P. W. Hayman, F. C. Romeijn and G. W. Van Oosterhout
Philips Res. Repts. 5 (1950) 173
- 15 J. R. Weertman and R. S. Averback
“Nanomaterials synthesis, Properties and Applications”
London Institute of Phys. Public. (1996) 323
- 16 B. S. Berly and W. C. Pritchett
Thin Solid Films 33 (1976) 19
- 17 G. W. Neiman, J. R. Weertman and R. W. Siegel
“Clusters and sluster assembled Materials”
Pittsburgh P. AMRS 206 (1991) 493
- 18 J. Rupp and R. Birringer
Phy. Rev. B 36 (1987) 7888
- 19 K. Lu
Scr. Metall. Mater. 25 (1994) 2047
- 20 H.Y. Tong, J. T. Wang, B. Z. Ding, H. G. Jiang and K. Lu
J. Non-cryst. Solids 150 (1992) 444
- 21 R. Birringer, U. Herr and H. Gleiter
Suppl. Trans. Jpn. Inst. Metals 2 (1986) 743
- 22 P. H. Buffat and J. P. Bord
Phys. Rev.A (1976) B 2287
- 23 J. Karch, R. Birringer and H. Gleiter
Nature (London) 330 (1987) 556
- 24 R. Birringer, U. Herr and H. Gleiter
Suppl. Trans. Jpn. Inst. Metals. (1986) 2743
- 25 A. E. Berkowitz, R. H. Kodama, S. S. Makhlof, F. T. Paarker, F. E. Spada, E. J. Jr. Meniff and S. Foner
J. Magn. Magn. Mater. 591 (1999) 196-197
- 26 C. Cannas, D. Gateschi, A. Musinu, G. Piccalunga and C. Sangregorio
J. Phys. Chem. B 102 (1998) 7721

- 27 H. Widatallah, C. Johnson, F. Berry and M. Pekala
Solid Stat. Commun. 120 (2001) 171-175
- 28 J. Lorimier, F. Bernard, O. Isnard, J. C. Niepce and J. F. Berar
Mater. Sci. Forum Vol. 378-381 (2001) 595-599
- 29 N. Ponpandian, P. Balaya and A. Narayanasamy
J. Phys. Condens. Matter. 14 (2002) 3221-3237
- 30 A. Chatterjee, D. Das, D. Chakravorty and K. Choudhury
Appl. Phys. Lett. 57 (1990) 1360-1362
- 31 Z. X. Tang, C. M. Sorensen and K. J. Klabunnde
Scr. Mater. 44 (1991) 1421-1424
- 32 M. Pal, P. Brahma, D. Chakravorty, D. Bhattacharya and H. S. Maiti
J. Magn. Magn. Mater. 164 (1996) 256-260
- 33 V. Šepelák, D. Baabe, D. Mienert, D. Schultze, F. Krumeich, F. J. Litterst and K. D. Becker
J. Magn. Magn. Mater. 257 (2003) 377-386
- 34 H. Nathani and R. D. K. Mishra
Mater. Sci. Engg. B 113 (2004) 228-235
- 35 H. Nathani, S. Gubbala and R. D. K. Mishra
Mater. Sci. Engg. B 121 (2005) 126-36
- 36 C. Caizer and M. Stefanescu
J. Phys. D: Appl. Phys. 35 (2002) 3035-3040
- 37 Petzold
J. Appl. Soft Magn. Nanocrystalline VITROPREM Alloys, J. de Physique IV 8 (2) (1998) 767-770
- 38 Y. Z. Li, L. Z. Ji and Z. H. G. Zhilm
Mater. Sci. Engg. B 9 (1999) 68-72
- 39 Y. Xu, Z. G. Liu, M. Umemoto and A. Tsuchiy
Metal. Mater. Trans. A 33 (2000) 2195

- 40 G. Caruntu, G. G. Bush and C. J. O'Connor
J. Mater. Chem. 14 (2004) 2753-2759
- 41 M. Gateshki, V. Petkov, S. K. Pradhan and T. Vogf
J. Appl. Cryst. 38 (2005) 727-779
- 42 G. Caruntu, I. Dumitru, G. G. Bush, D. Caruntu and C. J. O'Connor
J. Phy. Appl. Phys. 38 (2005) 811-815
- 43 L. D. Tung, V. Kolesnicherko, G. Caruntu, D. Caruntu, Y. Remond, V. O. Golub, C. J. O'Connor and L. Spinu
Physica B 319 (2002) 116-121
- 44 R. D. K. Misra, K. Sale, B. J. Kooi and J. Th. M. De Hosson
Mater. Sci. Techno. 19 (2003) 1617
- 45 G. P. Joshi, N. S. Saxena, R. Mangal, A. Mishra and T. P. Sharma
Bull. Mater. Sci. 26 (2003) 387-389
- 46 X. Feng, G. B. Pryxell, L. U. Wang, A. Y. Kim, J. Liu, R. M. Kemnerl
Science 276 (1997) 923
- 47 U. Bach, D. Lupo, P. Lomte, J. B. Moser, E. Weissortel, J. Sclbeck, H. Spreitzu and M. Gratzel
Nature (1998) 583
- 48 R. F. Ziole
U. S. Patent (1984) 4, 474, 866
- 49 R. H. Marchessault, Richards and P. Rioux
Carbohydrate Res. 224 (1992) 133.
- 50 R. D. McMichael, R. P. Shull, L. J. Swartzendruber, H. L. Bennett and R. E. Watson
J. Magn. Magn. Mater. 29 (1992) 111
- 51 I. Anton
J. Magn. Magn. Mater. 85 (199C) 219
- 52 P. Ravindernathan and K. C. Patil
J. Mater. Sci. 22 (1987) 3261

- 53 H. Igarash and K. Ohazaki
J. Am. Ceram. Soc. 60 (1997) 51
- 54 A. Goldman
J. Am. Ceram. Soc. Bull. 63 (1984) 582
- 55 D. Stoppels
J. Magn. Magn. Mater 160 (1996) 323
- 56 K. H. Lee, D. H. Cho and S. S. Jeung
J. Mater. Sci. Lett. 16 (1997) 83
- 57 C. S. Kim, Y. S. Yi, K. T. Park, H. Namgung and J. G. Lee
J. Appl. Phys. 85 (1999) 5223